Accurate Numerical Method for Calculating Frequency Distribution Functions in Solids. III. Extension to Tetragonal Crystals

Z. KAM AND G. GILAT
Department of Physics, Technion, Israel Institute of Technology, Haifa, Israel
(Received 10 June 1968)

The extrapolation method, initially developed by Gilat, Dolling, and Raubenheimer, has proved to be an accurate, rapid, and efficient method of calculating phonon densities of states in solids. In the present paper it is extended to tetragonal crystals and applied to white tin. The computation employs a Born–von Kármán model following Brovman and Kagan, and is based on recent experimental data by Rowe. The singularities appearing in the phonon density of states $g(\nu)$ are correlated to critical points predicted by the dispersion relations. It is found that six conspicuous singularities originate from off-symmetry directions. The resultant $g(\nu)$ is correlated to the tunneling data, and is employed for the calculation of specific-heat Debye temperature $\Theta_c(T)$.

I. INTRODUCTION

IN a preliminary paper by Gilat and Dolling,[1] an efficient method for calculating phonon densities of states was described. This method was further perfected in a later paper by Gilat and Raubenheimer[2] (hereafter referred to as I), and was applied to cubic crystals. In a more recent paper by Raubenheimer and Gilat[3] (hereafter referred to as II), this method was extended to hexagonal crystals and was applied to three hcp metals (namely, Be, Mg, and Zn). In the present paper, this method is extended to tetragonal crystals and is applied to β-Sn, which assumes this structure.

This calculation method is customarily referred to as the extrapolation method. It has already been adequately described in I and II, and only a brief summary is presented here. According to this method, the dynamical matrix[4] elements are calculated for a relatively small number of different wave vectors $\mathbf{q}_c$. At each of these $\mathbf{q}_c$ one computes the $3r$ eigenfrequencies $\nu_j(\mathbf{q}_c)$, where $j=1, 2, \cdots, 3r$, and r is the number of atoms in the primitive unit cell. In addition to the $\nu_j(\mathbf{q}_c)$ the gradients[5] $\nabla\nu_j(\mathbf{q}_c)$ are also calculated in order to perform a linear extrapolation for all the eigenfrequencies that can be obtained from a small volume ΔV located at $\mathbf{q}_c$. This extrapolation can be performed analytically by approximating the set of constant-frequency surfaces inside each of the volumes ΔV by a set of parallel planes which are perpendicular to $\nabla\nu_j(\mathbf{q}_c)$. This gives rise to a partial frequency distribution $g(j,\mathbf{q}_c,\nu)$ (see I and II), which when summed over all j and $\mathbf{q}_c$ yields the final $g(\nu)$. It should be noted, however, that the volumes ΔV must fill the irreducible part of the first Brillouin zone in an exhaustive manner. On the other hand, in order to simplify the logic of the calculation, it is desirable to set the shapes of ΔV so that they be as simple as possible. For the hexagonal lattice it is shown in II that it is possible to fill the irreducible zone by only two shapes, namely, rectangular and triangular prisms, respectively. Fortunately, the same procedure is also possible for the tetragonal lattice, and this greatly simplifies the calculations since all the analytical expressions required for the present case are already worked out in II.

The practical application of the method to β-Sn is described in Sec. II. In Sec. III we describe the force model employed for the calculation, and present the resultant dispersion relations for the high-symmetry directions, as well as for some other directions. In Sec. IV we bring the computed $g(\nu)$ and attempt a correlation between special points of the dispersion relations and singularities in $g(\nu)$. In addition, these singularities are compared to those observed in the superconducting tunneling data. A computation of the specific-heat Debye temperature is performed as well. The paper is summarized in Sec. V.

II. APPLICATION OF EXTRAPOLATION METHOD TO TETRAGONAL CRYSTALS

White tin (β-Sn) crystallizes in a tetragonal lattice with the space group D_{4h}^{19}. Its crystal structure can be represented by two interpenetrating body-centered Bravais lattices mutually displaced by a basis vector $(0,\frac{1}{2}a,\frac{1}{2}c)$, where a and c are the lattice parameters. The primitive cell of β-Sn therefore contains two atoms, and this implies that the dynamical matrix that de-

[1] G. Gilat and G. Dolling, Phys. Letters **8**, 304 (1964).
[2] G. Gilat and L. J. Raubenheimer, Phys. Rev. **144**, 390 (1966). A description of the FORTRAN procedure performing the computation of $g(\nu)$ is given by L. J. Raubenheimer and G. Gilat, Oak Ridge National Laboratory Report No. ORNL TM-1425, 1966 (unpublished).
[3] L. J. Raubenheimer and G. Gilat, Phys. Rev. **157**, 586 (1967). A descriptive report including the FORTRAN program for calculating $g(\nu)$ in hcp crystals is under preparation.
[4] Although the extrapolation method has so far been mainly applied to lattice-dynamical problems, it can be also applied in a straightforward manner to the calculation of other densities of states (e.g., electronic densities of states) as long as they are obtainable as distribution of eigenvalues of some energy matrix, which is a function of $\mathbf{q}$.
[5] A convenient method of obtaining the frequency gradients is a first-order perturbation calculation as described in I and II. There is, however, one case where the gradients are obtainable directly, and this is in the $\mathbf{k}\cdot\mathbf{p}$ method of electronic-energy-band calculation. This property speeds up considerably the calculation of $n(E)$ and was employed recently by C. W. Higginbotham, F. H. Pollack, and M. Cardona, Solid State Commun. **8**, 513 (1967).

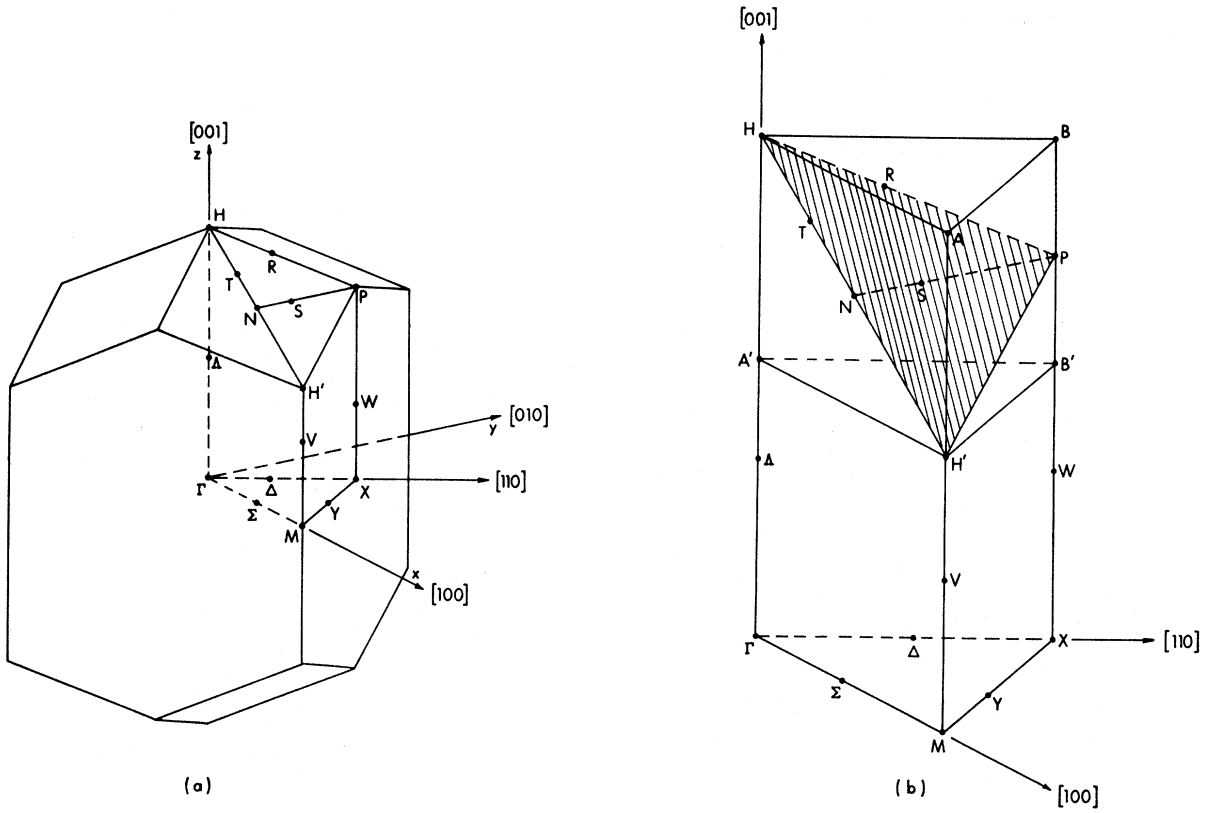

FIG. 1. (a) First Brillouin zone of tetragonal crystal for $\gamma_0=c/a<1$. (b) Practical zone throughout which the computation of $g(\nu)$ is carried out, as explained in the text.

scribes its vibrational properties must be of the order of 6×6.

The shape of the first Brillouin zone of tetragonal crystals depends on whether the c/a ratio is smaller or larger than 1. In this paper we treat only the case of $c/a<1$, since for β-Sn we have $c/a=0.544$ (at 110°K), but the case $c/a>1$ can be worked out along the same lines. In Fig. 1(a) we show the appropriate first Brillouin zone. The irreducible zone, which is $\frac{1}{16}$ in volume of the Brillouin zone, is included within the following five planes: $\Gamma HH'M$, ΓHPX, ΓMX, $MH'PX$, and $HH'P$. The shape of this irreducible zone is slightly less convenient in comparison to the irreducible zone of the hexagonal lattice. This is because, in contrast to the hexagonal case, the planes ΓMX and $HH'P$ are not parallel. It is possible, however, to get around this complication by slightly increasing the irreducible zone, so that it will take on a more convenient shape. This new shape, which is similar to that of the irreducible zone for the hexagonal case, is shown in Fig. 1(b). It is constructed by passing a plane HAB parallel to ΓMX. A little inspection reveals that the extra volume defined by the corners $HABPH'$ which is added to the irreducible zone is equivalent to the volume $HA'B'PH'$. This means that when one extrapolates throughout the volume defined by $HABH'A'B'$, which is the sum of these two equivalent volumes, one counts every point twice, and hence one must compensate for this by applying a weighting factor $W_{q_c}=0.5$ for all the points that happen to lie inside $HABH'A'B'$.

The more convenient volume over which we actually perform the linear extrapolation is now confined within the following five planes: ΓHAM, ΓHBX, ΓMX, $MABX$, and HAB. This volume, being somewhat larger than the irreducible zone, can be filled precisely by rectangular and triangular prisms in the same manner as the corresponding irreducible zone of the hexagonal case (see Fig. 2 of II). We refer to the zone as the practical zone. All the triangular prisms face the plane $MABX$, and their corresponding gradients lie in this plane.[6] The rest of the volume is filled only with rectangular prisms. Since a weighting factor of $W_{q_c}=0.5$ is used for part of the volume, as explained above, care must be taken to arrange the prisms in such a manner that the plane $H'A'B'$ does not intersect any of them. In the Appendix a short description is given of the way in which the practical zone is filled.

Having decided upon a certain simple procedure of filling the practical zone, it is now possible to proceed

[6] It is readily observed that the plane $MABX$, being a mirror plane, allows for extending the triangular prisms into rectangular prisms, so that half of their volume belongs to a neighboring irreducible zone. One can again readily correct for this "overfilling" by using a weighting factor $W_{q_c}=0.5$. In the present work, however, we used the triangular prisms.

in the same manner as in II (see also Appendix A of II) and to obtain the cross-section function $S(w)$ for the various prisms. The partial $g(j,\mathbf{q}_c,\nu)$ is now obtainable via Eq. (20) of I, where

$$W=0.5\ \mathbf{q}_c\in HABH'A'B' \\ =1.0\ \mathbf{q}_c\in MXH'A'B'. \quad (1)$$

III. FORCE MODEL AND DISPERSION RELATIONS

The main source of information for the interatomic force constants is the data of coherent inelastic scattering of neutrons. In the case of white tin a considerable body of data exists.[7] The most recent data, taken at 110°K, are those of Rowe.[8] β-Sn reveals quite an intricate structure in the phonon data which suggests a strong electron-phonon interaction.[8] This interaction is observed in the phonon spectrum as Kohn anomalies whenever $\mathbf{q}$ connects two opposite points on the Fermi surface. Now the Fermi surface of β-Sn extends to at least the fifth Brillouin zone,[9] and this is compatible with the intricate structure of the phonon spectrum. It seems that it would be quite hopeless to try to represent the data adequately by a Born–von Kármán force model which does not include many neighbors. This fact was observed by Rowe,[8] who abandoned such an attempt. Hopefully, a better approach might be made by attempting a pseudopotential calculation, based, for example, on a model potential, as suggested by Heine, Abarenkov, and Animalu[10] and recently reformulated by Shaw and Harrison.[11]

Although we do not expect a very satisfactory representation of the data by a Born–von Kármán model, we nevertheless proceed and work out a best fit to such a model. Our motive for doing so is that the objective of this work is a specific one—the application of the accurate numerical technique for obtaining the phonon density of states. We believe that it is of considerable interest and importance to obtain a better understanding of the structure of the singularities in the frequency distribution, and this can be achieved by correlating it to some relatively simple force model.[12] The Born–von Kármán model employed by us is based on a paper by Brovman and Kagan (BK).[13] The force model of BK includes interactions between neighbors up to the sixth nearest neighbor. They list the dynamical matrix elements at a general wave vector $\mathbf{q}$. This matrix element $D_{\alpha\beta}(\kappa\kappa',\mathbf{q})$, where κ, $\kappa'=1$, 2 label the two atoms in the primitive cell, assumes the general form

$$D_{\alpha\beta}(11)=D_{\alpha\beta}{}^*(22), \\ D_{\alpha\beta}(12)=D_{\alpha\beta}{}^*(21). \quad (2)$$

In their practical calculation BK impose certain restrictions on their set of force constants. Of the total set of 24 force constants for a first- through sixth-neighbor model, they use only 14 independent parameters. Two force constants can be eliminated by imposing the Born-Huang equilibrium conditions. Eight more parameters are deleted by assuming that interactions with third through sixth neighbors assume axial symmetry and can thus be described by six force constants rather than 14. The force constants describing the interactions of the first through third neighbors are of tensorial nature. This is so because of the pronounced covalent nature of the binding in β-Sn. The restrictions imposed on the force constants simplify to some extent the nature of the dynamical matrix, and under these conditions the elements of the submatrices $D_{\alpha\beta}(11)$ and $D_{\alpha\beta}(22)$ become real, and hence

$$D_{\alpha\beta}(11)=D_{\alpha\beta}(22). \quad (3)$$

Because of this relation it is possible to transform the whole of the dynamical matrix into a real and symmetric matrix M. This is achieved by applying a unitary transformation V, given by

$$\mathbf{V}=\frac{1}{\sqrt{2}}\begin{vmatrix}\mathbf{I} & i\mathbf{I}\\ i\mathbf{I} & \mathbf{I}\end{vmatrix}, \quad (4)$$

where $\mathbf{I}$ is a 3×3 unit matrix. $\mathbf{M}$ is then given by

$$\mathbf{M}(\mathbf{q})=\begin{bmatrix}\mathbf{D}(11)-\mathrm{Im}\mathbf{D}(12) & \mathrm{Re}\mathbf{D}(12)\\ \mathrm{Re}\mathbf{D}(12) & \mathbf{D}(11)+\mathrm{Im}\mathbf{D}(12)\end{bmatrix}. \quad (5)$$

Unfortunately, it was impossible for us to make use of the numerical values of the force constants given by BK.[13] The reason for this is evidently some calculation error that exists in this paper and which shows up on trying to compare the graph of the calculated phonon dispersion relations (Fig. 3 of Ref. 13) to the numerical values of the force constants (Table II of Ref. 13). Therefore we had to take the BK model as a general basis for a best-fit analysis. In doing so, we dispensed with its equilibrium conditions and employed it as a best-fit formula to the experimental phonon dispersion relations of Rowe.[8] Being aware that it

[7] D. Long-Price, in *Inelastic Scattering of Neutrons* (International Atomic Energy Agency, Vienna, 1965), Vol. I, p. 109; G. Borgonovi, G. Caglioti, and M. Antonini, *ibid.*, Vol. I, p. 117; R. E. Schmunk and W. R. Gavin, Phys. Rev. Letters **14**, 44 (1965); J. M. Rowe, B. N. Brockhouse, and E. C. Svensson, *ibid.* **14**, 583 (1965).

[8] J. M. Rowe, Phys. Rev. **163**, 547 (1967).

[9] G. Weisz, Phys. Rev. **149**, 504 (1966).

[10] I. V. Abarenkov and V. Heine, Phil. Mag. **12**, 529 (1965); V. Heine and I. V. Abarenkov, *ibid.* **9**, 451 (1964); A. O. E. Animalu, *ibid.* **11**, 379 (1965); and A. O. E. Animalu and V. Heine, *ibid.* **12**, 1249 (1965).

[11] R. W. Shaw and W. A. Harrison, Phys. Rev. **163**, 604 (1967).

[12] Since the present method of calculations is by no means restricted to Born–von Kármán models, we hope to apply it in due time to a more physical model, as given, for example, in Refs. 10 and 11.

[13] E. G. Brovman and Yu. Kagan, Fiz. Tverd. Tela **8**, 1402 (1966) [English transl.: Soviet Phys.—Solid State **8**, 1120 (1966)].

TABLE I. List of the force constants obtained from a best-fit calculation to the data of Rowe (Ref. 8). The notation is that of Brovman and Kagan (Ref. 13).

Force constant	Value (in units of 10^8 dyn/cm)	Neighbor number	Multiplicity of neighbors	Distance from origin	Relations imposed by axial symmetry
α_1	28.78	1	4	$\frac{1}{4}(4a^2+c^2)^{1/2}$	none
β_1	−6.26				
γ_1	−1.76				
δ_1	16.64				
α_2	22.08	2	2	c	none
β_2	0.00				
α_3	2.28	3	3	$\frac{1}{4}(4a^2+9c^2)^{1/2}$	none
β_3	3.88				
γ_3	3.60				
δ_3	−7.48				
α_4	0.82	5	8	$\frac{1}{2}(2a^2+c^2)^{1/2}$	...
β_4	0.34				...
γ_4	0.67				$\gamma_4=(\alpha_4-\beta_4)/(1-\gamma_0^2)$
σ_4	0.67				$\sigma_4=\gamma_4$
δ_4	0.37				$\delta_4=\gamma_0(\alpha_4-\beta_4)/(1-\gamma_0^2)$
ϵ_4	0.37				$\epsilon_4=\delta_4$
α_5	0.39	5	4	$\frac{1}{4}(4a^2+25c^2)^{1/2}$	
β_5	0.58				
γ_5	0.23				$\gamma_5=(25/4)\gamma_0^2(\alpha_5-\beta_5)+\beta_5$
δ_5	−0.26				$\delta_5=\frac{5}{2}\gamma_0(\alpha_5-\beta_5)$
α_6	2.53	6	4	a	...
β_6	0.94				...
γ_6	0.94				$\gamma_6=\beta_6$
δ_6	0.00				$\delta_6=0$

would be difficult to obtain a good empirical representation of the data where they show considerable complexity [i.e., for $0.4<\zeta<0.7$ along the $[00\zeta]$ direction, $q_z=(2\pi/c)\zeta$], we gave up such an attempt and focused our attention on those parts of the phonon spectrum where the fine structure is less pronounced. In Table I we present the numerical results for our model. In Fig. 2 we present the computed dispersion relations in solid lines. The wave vector ζ is given in reduced units, i.e.,

$$(2\pi/a)\zeta=(q_x,q_y,\gamma_0 q_z), \tag{6}$$

where $\gamma_0=c/a$, and the units of $\mathbf{q}$ are $(2\pi/a,\ 2\pi/a,\ 2\pi/c)$.

The data are in good agreement (better than 5%) with the model for most of the branches over all the range where the experimental data exist. The notable exception is, as expected, for the Λ_1 and Λ_3 modes (LA and LO) along the $[00\zeta]$ direction in the range $0.4<\zeta<0.7$. The classification of modes of vibration follows Chen,[14] who analyzed the lattice dynamics of β-Sn by group-theoretical methods. Apart from the customary high-symmetry directions Λ, Σ, and Δ we bring also in Fig. 2 the branches along the directions Y and W. Along these directions we have only three separate branches, each doubly degenerate.[14] In addition to the high-symmetry directions we present dispersion relations along the directions HN, NP, and PH, which we label by R, S, and T, respectively. We have a few reasons for presenting these additional dispersion relations which are of lower symmetry. In the first place, it is interesting to have an idea of the behavior of $\nu_j(\mathbf{q})$ in the vicinity of the point N, which is of high symmetry. It is, for instance, a center of inversion for the reciprocal lattice. As a result of this property, the gradients of $\nu_j(\mathbf{q})$ at N must vanish, and this fact should show up in $g(\nu)$ as Van Hove singularities. Apart from this, the same property makes the lines HNH' and PN (R and S, respectively) mirror lines in the plane HPH'. In view of this last characteristic, the line PN itself, for which $q_z=\pi/c$, becomes an inversion line, so that any extremum in the branches of its dispersion relations should be a genuine critical point, and hence show up in $g(\nu)$. In addition to these reasons we also find that the highest frequency that appears in the total irreducible zone happens to be along the T direction (HP) and it has the value $\nu(0.38,\ 0.38,\ 0.53)=4.71\times10^{12}$ cps.

The branches in Figs. 2 and 3 are labeled according to the group-theoretical classification.[14] In the case that more than one branch belongs to a representation, we classify these branches with an additional label A or O so that A labels the lowest branch and O_i labels higher branches in a decreasing order: O_1 marks the highest, O_2 the second highest, etc. The same mode of labeling was adopted in II.

In the calculation of the best-fit model we made use only of the inelastic neutron scattering data of Rowe.[8] As a result, the acoustic branches at Γ tend to have somewhat smaller slopes when compared to the veloci-

[14] S. H. Chen, Phys. Rev. 163, 532 (1967); also Ph.D. thesis, McMaster University, 1964 (unpublished).

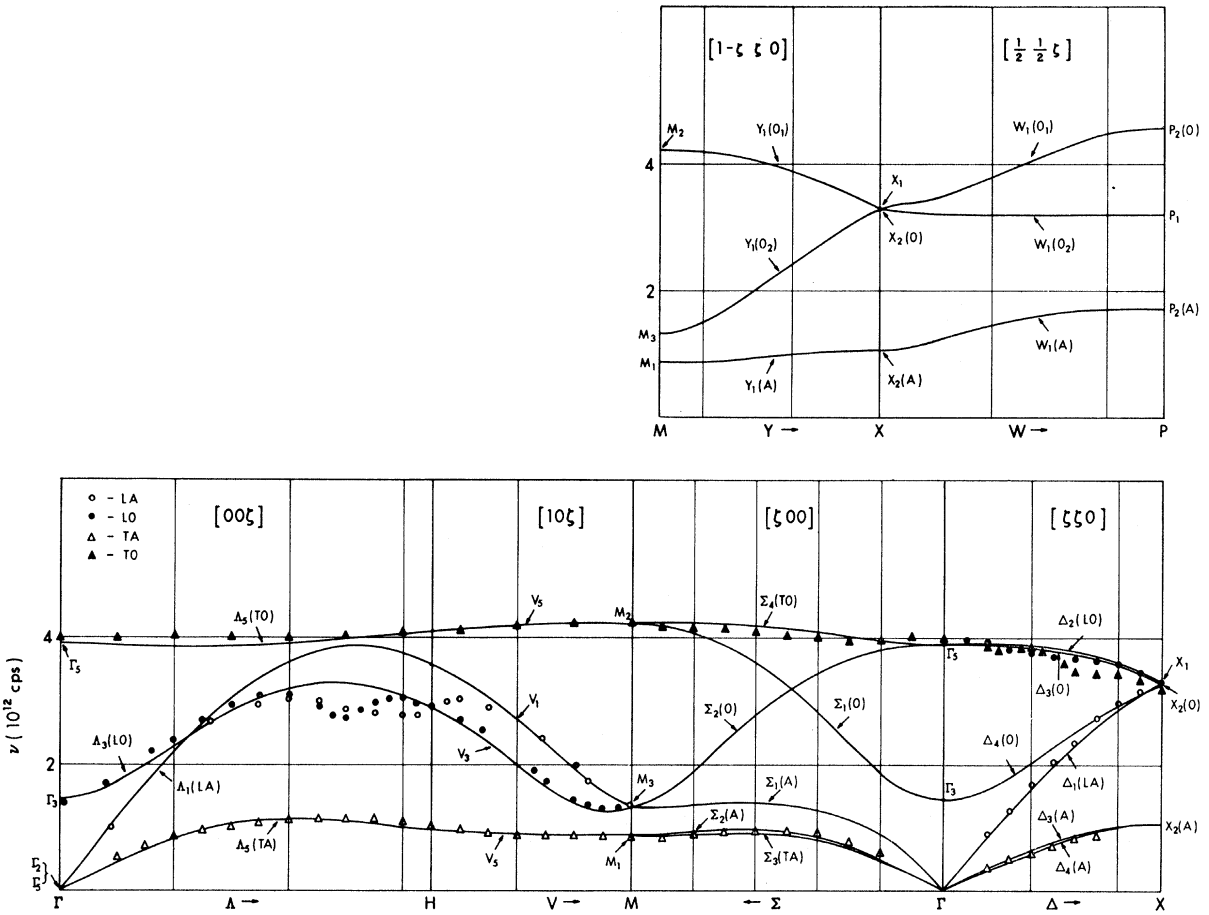

FIG. 2. Phonon dispersion relation along high-symmetry directions in white tin based on a first-through-sixth neighbor Born–von Kármán model. The experimental points are taken from Rowe (Ref. 8). The classification of modes follows Chen (Ref. 14).

ties of sound measured by Rayne and Chandrasekhar.[15] This discrepancy of about 5% might affect to some extent the Debye end of $g(\nu)$, and corrective steps are required in order to obtain a good fit to the low-temperature specific-heat data. This point is further treated in Sec. IV.

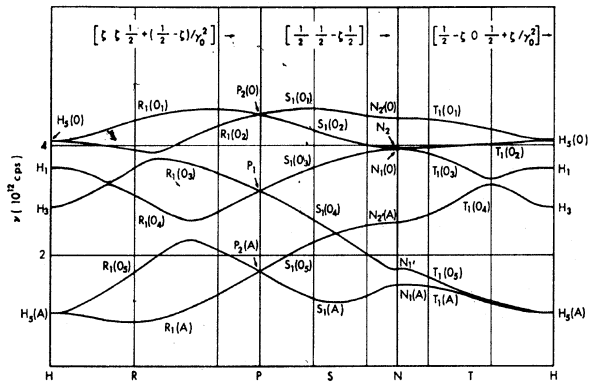

FIG. 3. Phonon dispersion relations along three lower-symmetry directions in the plane HPH' (see Fig. 1). The classification of modes is described in the text.

IV. CALCULATION OF $g(\nu)$ AND DERIVED PROPERTIES

Having obtained a force model and the phonon dispersion relations, we proceed to compute $g(\nu)$, the phonon frequency distribution function. The method of filling the practical zone is described in Sec. I, where the practical zone is shown in Fig. 1(b). The mesh of points at which we solve the secular equation to obtain $g(j,\mathbf{q}_c;\nu)$ is schematically given[3] in II. The points $\mathbf{q}_c$ are as evenly distributed as possible. Some care must be taken, however, for the following reason: Throughout the volume $HABH'A'B'$ we use a weighting factor $W_{\mathbf{q}_c}=\frac{1}{2}$, whereas the weighting factor is 1 for the rest of the volume. Therefore, one must choose the points $\mathbf{q}_c$ on each side of the plane $H'A'B'$ in such a manner that the faces of the prisms (rectangular and triangular) exactly touch this plane on both sides. This is important in order to guarantee that only a single weighting

[15] J. A. Rayne and B. S. Chandrasekhar, Phys. Rev. **120**, 1658 (1960).

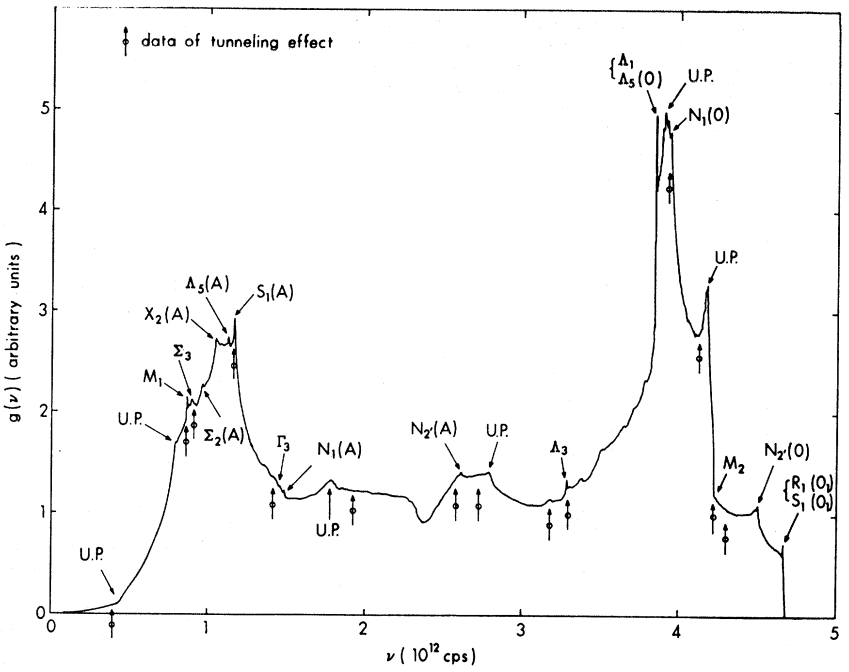

FIG. 4. Frequency distribution function for white tin derived from a Born–von Kármán model. Singularities that can be correlated to critical points in the phonon dispersion relations are indicated according to their classification. Singularities which cannot be predicted from dispersion relation are indicated by U.P. Critical points observed by Rowell and Kopf (Ref. 17) in the tunneling effect are denoted by arrows.

factor is used for each prism. In the Appendix we describe more quantitatively the way of choosing $\mathbf{q}_c$. In our actual calculation we diagonalized the dynamical matrix at 2565 different values of $\mathbf{q}_c$ over the practical zone [Fig. 1(b)]. Then we computed $g(\nu)$, as described[2,3] in I and II. The resultant $g(\nu)$ is shown in Fig. 4, and it is an exact copy of a computer plot. $g(\nu)$ is sorted into frequency intervals $(\nu, \nu+d\nu)$ of the size $d\nu=0.0025\times10^{12}$ cps, so that almost 2000 different values of $g(\nu)$ are used in the plot of Fig. 4. This provides for a resolution 50 times better than that given by *BK*.[13] A few striking features of $g(\nu)$ are worth mentioning. Most notable is the singularity observed at $\nu_1=0.44\times10^{12}$ cps, which originates from an off-symmetry direction at $\zeta=(0.78, 0.19, 0.15)$. This singularity limits the range of the Debye approximation of $g(\nu)$ to frequencies smaller than ν_1, which is less than 10% of the total range of frequencies. This critical point is probably the reason for the very sharp drop in the characteristic $\Theta_c(T)$ of the specific heat C_V observed in β-Sn in the range 0–10°K. The value of ν_1 in °K is about 20°K, but its effect should begin to show up at lower temperatures. A similar feature is observed also for zinc.[3] There is a singularity there at $\nu=1.37\times10^{12}$ cps which limits the Debye approximation for a range which is roughly 20% of the total range. The resultant $\Theta_c(T)$ for Zn shows a similar drop, which reaches a deep minimum at 20°K. This behavior has recently been reported experimentally by Martin.[16]

As expected, the calculated $g(\nu)$ for β-Sn as shown in Fig. 4 has many more fine details than those given by BK. We attempt to correlate the various singularities in $g(\nu)$ to the expected critical points, as predicted by the dispersion relations given in Figs. 2 and 3. Whenever such a correlation is found, it is indicated on the plot of $g(\nu)$. In Table II we list all the expected critical points. The degree to which they show up in the curve of $g(\nu)$ is classified in a somewhat subjective way into three classes—*s*, *w*, and *a*. *s* stands for strong, *w* for weak, and *a* for absent. In addition to these critical points we list another six conspicuous singularities in $g(\nu)$ which arise from off-symmetry points. Among these singularities is ν_1. These points are marked on the graph by U.P. (unpredicted). We attempt also to correlate the singularities found in $g(\nu)$ to those observed in the experimental graph of d^2V/dI^2 versus V in the tunneling experiment of β-Sn. These last singularities are marked by arrows in Fig. 4. The listing of these singularities is given by Rowe,[8] who too attempts such a correlation. To this list we added one more frequency at $\nu=0.39\times10^{12}$ cps (1.6 meV), which can be observed in the structure of d^2V/dI^2 in the data of Rowell of Kopf.[17] The fit of the structure of the tunneling data to that of the calculated density of states is good in a few cases, as can be observed in Fig. 4. It is not very surprising that the fit is not better in view of the crudeness of our model and the somewhat vague interpretation of the tunneling data. Moreover, in a recent paper by Dynes *et al.*[18] a similar correlation of such data in the case of lead is discussed. They deduce from their analysis that critical points obtained from off-symmetry directions via the Born–von Kármán force model might be

[16] D. L. Martin, Phys. Rev. **167**, 640 (1968).

[17] J. M. Rowell and L. Kopf, Phys. Rev. **137**, A907 (1965).

[18] R. C. Dynes, J. P. Carbotte, and E. J. Woll, Jr., Solid State Commun. **6**, 101 (1968).

TABLE II. List of Van Hove critical points predicted from the dispersion relations (Figs. 2 and 3). In column 3 the topological nature of the point is given (M means maximum, m is minimum, and I encompasses all other cases with zero gradient). In column 4 we specify the strength of the singularity [s stands for strong, w for weak, and a indicates the absence of the singularity in $g(\nu)$].

Assignment	ν (10^{12} cps)	Nature	Strength
$\Lambda_5(A)$	1.130	M	s
M_1	0.867	m	s
Γ_3	1.459	m	$w(a)$
Λ_3	3.288	M	s
V_3	1.255	m	a
Λ_1	3.855	M	s
$\Lambda_5(O)$	3.851	m	s
M_2	4.224	M	s
$\Sigma_2(A)$	0.965	M	s
Σ_3	0.906	M	s
$\Sigma_1(A)$	1.380	M	a
Γ_5	3.904	I	w
$X_2(A)$	1.064	I	s
$N_1(A)$	1.492	M	s
$N_{1'}$	1.745	I	a
$N_{2'}(A)$	2.620	I	s
$N_1(O)$	3.957	M	s
N_2	3.971	m	a
$N_{2'}(O)$	4.509	I	s
$R_1(O_1)$	4.670	M	s
$S_1(O_1)$	4.670		
$S_1(A)$	1.167	I	s
unpredicted	0.443		s
	0.800		s
	1.785		s
	2.800		s
	3.915		s
	4.178		s

wrong, and one must either look for a better model or obtain these points experimentally by measuring $\nu_j(\mathbf{q})$ at off-symmetry $\mathbf{q}$ vectors.

Knowing $g(\nu)$, the calculation of $\Theta_c(T)$ is straightforward. In view of the lack of good fitting of our model to the slopes of the acoustic modes given by the appropriate velocities of sound,[15] we renormalized the Debye end of $g(\nu)$ to account for this. It is obvious that $\Theta_c(0)$ is solely determined by the elastic constants. The value of $\Theta_c(0)$ appropriate for the elastic constants measured at 110°K can be obtained from the data of Rayne and Chandrasekhar,[15] and it is $\Theta_c(0)=192\pm3$°K. We used this value to renormalize $g(\nu)$ in the range $0<\nu<0.3\times10^{12}$ cps. This renormalization cannot affect significantly the rest of the spectrum, and as a matter of fact it is too small to be observed on the graph of $g(\nu)$. The calculated $\Theta_c(T)$ is shown in Fig. 5, together with the experimental $\Theta_c(T)$ as reported by De Sorbo.[19] As expected, the calculated $\Theta_c(T)$ fits well the experimental data at $T=0$°K. Both data show the deep drop in $\Theta_c(T)$ at $T=9$°K, but the calculated graph predicts a somewhat deeper minimum. The over-all fit is considered satisfactory in view of the crudeness of the model. We find the $\Theta_s(T)$ for the entropy to be $\Theta_s(T)=155$°K at $T=110$°K.

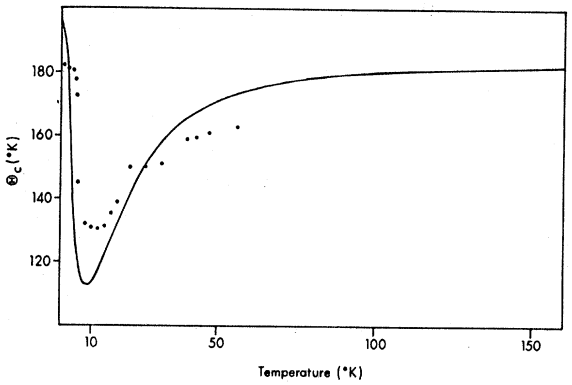

FIG. 5. Calculated specific-heat Debye temperature $\Theta_c(T)$ for white tin. Experimental points are taken from De Sorbo (Ref. 19).

V. SUMMARY

In the present paper we are mainly interested in the extension and application of the extrapolation method to tetragonal crystals. In view of this, the problem of providing a satisfactory force model to β-Sn becomes of secondary importance. In saying this we do not mean to belittle the importance of this problem, which deserves a thorough investigation. But we want to focus attention on the specific objective of this work, as indicated by its title. Because of this we have not attempted to produce the best possible model, but rather to find one which is able to represent the experimental data reasonably well. We are quite aware of the shortcomings of our model, and in principle of any Born–von Kármán model, as indicated by Rowe.[8] Nevertheless, we are positive that there is still wide room for a better understanding of the correlation between a given force model and the frequency distribution function derived from it. Existing calculations of frequency distributions for β-Sn are quite rare, and the few existing ones lack the fine features of singularities that can be displayed convincingly by the application of the present method. Moreover, this method becomes potentially more powerful for a more complicated crystal structure. This is so in the sense of its capacity for displaying fine features of the spectrum within a relatively short numerical computation. It is believed that in its present stage this method preserves all the information associated with a given force mode. In contrast, earlier calculation methods could show only the coarser features of the spectrum.

In the present paper no basic new developments are added to those presented in I and II. The problem of computing the phonon density of states for tetragonal symmetry is conveniently solved by slightly enlarging the irreducible zone, so that it resembles the shape of the hexagonal irreducible zone already discussed in II. We compensate for this enlargement by employing a suitable weighting factor. Presumably the same tech-

[19] W. De Sorbo, Acta Met. 2, 274 (1954).

nique can be applied in the case of lower symmetries, so that the shape of their irreducible zone is enlarged in order to make it similar to some irreducible zone of an already solved case. This could save a considerable amount of work in finding the cross-section area of more complicated geometrical shapes.

In the special case of β-Sn a correlation of the critical points predicted from the dispersion relations to the singularities in the phonon density of states is attempted. Many singularities can be correlated in an obvious manner. Some predicted critical points do not show up in $g(\nu)$. Moreover, we find six strong singularities in $g(\nu)$ that originate from off-symmetry wave vectors. A similar finding was reported in II for the case of hexagonal crystals.

In view of the weaknesses of our force model we refrain from emphasizing the physical conclusion derivable from the present calculation. Nevertheless, the results are compared to the superconducting tunneling data as well as the specific-heat data with considerable success. It is hoped that if a better model were employed, the fit could be of more significance.

APPENDIX

In this Appendix a short description of the method of generating the mesh of points $\mathbf{q}_c$ is given. As mentioned in Sec. II, care must be taken to ensure that the plane $H'A'B'$ in Fig. 1(b) does not intersect any of the prisms. We therefore choose two different integers, N_{1z} and N_{2z}, to divide the practical zone along the z axis. In the volume confined between the parallel planes ΓMX and $H'A'B'$ we have N_{1z} "layers" of prisms for the weighting factor $W_{\mathbf{q}_c}=1$. In the remainder of the volume confined between the parallel planes $H'A'B'$ and HAB there are N_{2z} such layers, and the weighting factor attached to each of them is $W_{\mathbf{q}_c}=\frac{1}{2}$. The x axis is divided into N_x segments, and so is the y axis. Let n_x and n_y be positive integers satisfying $1\leqslant n_y\leqslant n_x\leqslant N_x$ and let n_{1z} and n_{2z} be other positive integers satisfying $1\leqslant n_{1z}\leqslant N_{1z}$ and $1\leqslant n_{2z}\leqslant N_{2z}$; then the coordinates of a mesh point q_c are given by

$$q_{cx}=(\pi/aN_x)(n_x+n_y-1),\quad 1\leqslant n_y\leqslant n_x\leqslant N_x$$

$$q_{cy}=(\pi/aN_x)(n_x-n_y),$$

$$q_{cz}=(\pi/cN_{1z})(1/\gamma_0-\gamma_0)(n_{1z}-\tfrac{1}{2}),\quad \text{for } 1\leqslant n_{1z}\leqslant N_{1z},\quad W_{\mathbf{q}_c}=1$$

$$=(\pi/cN_{1z})(1/\gamma_0-\gamma_0)(N_{1z}-\tfrac{1}{2})+(2\pi/cN_{2z})\gamma_0(n_{2z}-\tfrac{1}{2}),\quad \text{for } 1\leqslant n_{2z}\leqslant N_{2z},\quad W_{\mathbf{q}_c}=\tfrac{1}{2}.$$

Although there are no restrictions on the choice of N_x, N_{1z}, and N_{2z}, we prefer to choose them in such a manner that the practical zone is filled by mesh points as evenly as possible. In order to achieve this, N_x, N_{1z}, and N_{2z} are so chosen that the ratio $N_x: N_{1z}: N_{2z}$ is as close as possible to the ratio $\sqrt{2}: (1/\gamma_0-\gamma_0): 2\gamma_0$, where $\gamma_0=c/a$. The total number of mesh points in the practical zone is given by

$$N=\tfrac{1}{2}N_x(N_x+1)(N_{1z}+N_{2z}).$$

Note added in proof. It was pointed out to us by Dr. L. J. Raubenheimer that the practical zone could be made smaller by passing a plane parallel to ΓMX through the point N in Fig. 1(b). By doing so the number of points at which one solves the dynamical matrix becomes somewhat smaller, and the weighting factor $W_{\mathbf{q}_c}$ could be set equal to 1 throughout all the zone.